Article

Current Biology

# Transcranial magnetic stimulation effects support an oscillatory model of ERP genesis

## Graphical abstract

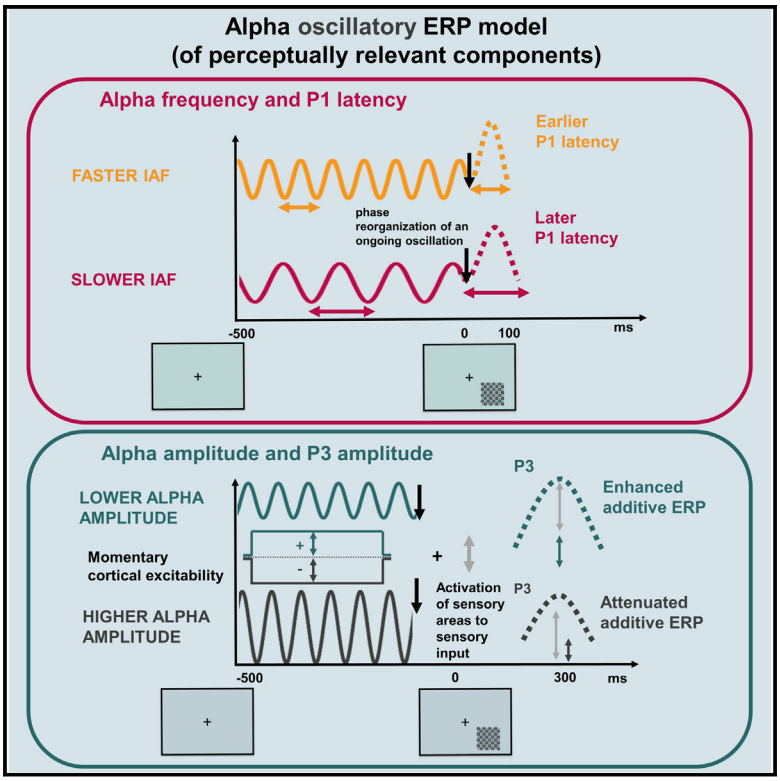


## Highlights

- Prestimulus alpha oscillations contribute to the generation of post-stimulus ERPs
- Individual alpha frequency predicts the latency of the P1 component
- Alpha amplitude predicts the size of the P3 response
- These mechanisms have distinct behavioral links (visual accuracy vs. confidence)

## Authors

Jelena Trajkovic, Francesco Di Gregorio, Gregor Thut, Vincenzo Romei

## Correspondence

vincenzo.romei@unibo.it

## In brief

Trajkovic et al. propose an alpha oscillatory model of ERP genesis. By using rhythmic TMS-EEG, they offer causative evidence that individual alpha frequency determines the latency of the earlier P1 component, related to perceptual accuracy, while alpha amplitude shapes the size of the later P300 response, related to subjective confidence ratings.

Trajkovic et al., 2024, Current Biology *34*, 1048–1058
March 11, 2024 
https://doi.org/10.1016/j.cub.2024.01.069

CellPress

CellPress
OPEN ACCESS

Current Biology

Article

# Transcranial magnetic stimulation effects support an oscillatory model of ERP genesis

Jelena Trajkovic,[1,2] Francesco Di Gregorio,[1] Gregor Thut,[3] and Vincenzo Romei[1,4,5,6,*]
[1]Centro studi e ricerche in Neuroscienze Cognitive, Dipartimento di Psicologia, Alma Mater Studiorum – Università di Bologna, Campus di Cesena, Cesena 47521, Italy
[2]Department of Cognitive Neuroscience, Faculty of Psychology and Neuroscience, Maastricht University, 6229 ER Maastricht, the Netherlands
[3]Centre for Cognitive Neuroimaging, School of Psychology and Neuroscience, MVLS, University of Glasgow, Glasgow G128QB, UK
[4]Facultad de Lenguas y Educación, Universidad Antonio de Nebrija, Madrid 28015, Spain
[5]X (formerly Twitter): @VincenzoRomei
[6]Lead contact
*Correspondence: vincenzo.romei@unibo.it
https://doi.org/10.1016/j.cub.2024.01.069

## SUMMARY

Whether prestimulus oscillatory brain activity contributes to the generation of post-stimulus-evoked neural responses has long been debated, but findings remain inconclusive. We first investigated the hypothesized relationship via EEG recordings during a perceptual task with this correlational evidence causally probed subsequently by means of online rhythmic transcranial magnetic stimulation. Both approaches revealed a close link between prestimulus individual alpha frequency (IAF) and P1 latency, with faster IAF being related to shorter latencies, best explained via phase-reset mechanisms. Moreover, prestimulus alpha amplitude predicted P3 size, best explained via additive (correlational and causal evidence) and baseline shift mechanisms (correlational evidence), each with distinct prestimulus alpha contributors. Finally, in terms of performance, faster prestimulus IAF and shorter P1 latencies were both associated with higher task accuracy, while lower prestimulus alpha amplitudes and higher P3 amplitudes were associated with higher confidence ratings. Our results are in favor of the oscillatory model of ERP genesis and modulation, shedding new light on the mechanistic relationship between prestimulus oscillations and functionally relevant evoked components.

## INTRODUCTION

Intrinsic ongoing brain oscillations represent more than mere background noise; a growing number of theoretical and empirical works support the notion that oscillatory activity plays an active role in cognitive and perceptual performance.[1–5] For instance, the findings that prestimulus oscillations—capturing ongoing activity before any stimulus is presented—predict perceptual performance is in support of this view.[6–12] By affirming a functional significance of ongoing (e.g., prestimulus) oscillations that goes beyond "random noise" and thus play a crucial role in shaping sensory and cognitive processes, it becomes tempting to infer that these oscillations must also play an essential role in shaping post-stimulus event-related potentials (ERPs).[13] By extension, this also casts doubts on the "evoked model" of ERPs that posits a strict distinction between ERPs—conceived as a stimulus-evoked response of constant latency and polarity—and ongoing electroencephalographic (EEG) activity.[14,15] The alternative view, known as the "oscillatory model," states that, at least in part, evoked responses are generated from a reorganization of ongoing brain oscillations, contradicting a complete independence between background EEG and ERPs.[14] In other words, the oscillatory model posits that oscillations can influence the generation of the ERP components in some way (e.g., via phase reorganization, baseline shift, a change in frequency, or intrinsic brain state), while the evoked model assumes their complete independence.

What is the proposed mechanism explaining the generation of ERPs in the oscillatory model? Some studies have suggested that, with stimulus presentation, oscillations of different frequencies undergo resetting and, as a result, become synchronized in their absolute phase after stimulus onset, thus producing ERP components.[14,16–21] In line with this view, it was shown that brain oscillations across different frequency ranges sustain phase reset to become synchronized within the time window of the P1-N1 complex.[17–19] However, due to methodological difficulties in separating the two proposed models, most of the arguments and predictions used to dissociate the evoked and the oscillatory (phase-resetting) model have proven inconclusive. As a result, research has failed to agree on the exact origins of ERPs.[13]

In the two-decades-long debate on the origin of ERPs through phase reorganization, there has been an emphasis on a possible association between ongoing oscillatory activity in the alpha frequency band (8–12 Hz) and visual-evoked components. It has been suggested that such an association is conceivable, given

 

that perceptually relevant ongoing oscillations in the alpha band and ERPs share frequency characteristics and amplitude relationships.[13] However, in contradiction with this claim, it has been demonstrated that the phase of oscillatory alpha activity is preserved after stimulus onset relative to its prestimulus phase, thus questioning phase-resetting of alpha activity as a primary generator of visual ERPs.[15] Based on these results, the authors argue that ERPs and ongoing oscillations could represent separate neuronal events, leaving, however, the possibility open that prestimulus alpha oscillations can modulate the generation of ERPs, in line with findings that they can modulate perception.[6–12,22–29] To explain these latter findings, influential theories have proposed an active role of alpha oscillations in sensory processing, where the neural synchronization in the alpha range could represent a momentary index of visual cortex excitability[10,11,30,31] and the alpha phase could represent pulsed inhibition,[32,33] parceling incoming information into discrete samples.[34] Moreover, recent evidence from our group shed light on the perceptual implications of prestimulus alpha frequency as opposed to alpha amplitude.[7] We used EEG to measure prestimulus alpha oscillations during a visual detection task, which were then entrained online using rhythmic transcranial magnetic stimulation (rhTMS) over the occipital cortex. We found that controlling alpha frequency by rhTMS modulates perceptual accuracy but not subjective confidence, while enhancing alpha amplitude reduces confidence but not accuracy.[7] These findings provided causal evidence of a double dissociation between alpha frequency and alpha amplitude, linking alpha frequency to the neural pace of information sampling,[22,24,35–37] and alpha amplitude to the level of neural excitability and conscious access to both signal and noise.[6,8,9,12]

Here, we build on this recent finding of a dissociable, causal role of alpha frequency and alpha amplitude in conscious perception to test the oscillatory model of ERP genesis. If different aspects of prestimulus brain oscillations causally modulate different aspects of perceptual performance, such as accuracy and awareness, and the oscillatory model applies, then entraining these oscillations should also modulate post-stimulus ERPs along their functional association with these perceptual performance measures. Specifically, we hypothesized that if the oscillatory model is correct, then controlling prestimulus alpha oscillations in their frequency and amplitude through rhTMS will differently affect early and late post-stimulus ERP components, such as the C1/P1 vs. the P3. This is because C1 and P1 are mainly generated in striate and extrastriate visual areas[38] and should hence more directly reflect the degree of sensory evidence and, by extension, be associated with accuracy. By contrast, the P3 is of a centro-parietal origin and has been related to sensory readout for decision-making[39] and subjective awareness/consciousness of a stimulus[40,41] rather than the level of sensory evidence[42] and hence should be associated more with a subjective appraisal of perception. Hence, we expected that by controlling prestimulus alpha frequency through rhTMS, we would modulate the efficiency of sensory processing, both neurally and in terms of performance (e.g., observe earlier C1/P1 latencies and/or higher C1/P1 amplitudes with faster prestimulus alpha frequency, alongside enhanced accuracy). On the other hand, we expected that controlling prestimulus alpha amplitude through rhTMS would influence the later P3 component (latency or amplitude) as part of a mechanism that shapes subjective stimulus evaluation.

Here, we first tested the existence of a correlative relationship between prestimulus alpha frequency, the C1/P1 components, and perceptual accuracy on the one hand, and prestimulus alpha amplitude, P3 component and perceptual confidence, on the other hand by means of EEG recording during a perceptual task (experiment 1). Second, non-invasive brain stimulation was used to causally test the two models of ERP genesis by directly probing for a causal dissociation of different parameters of alpha activity in the genesis of distinct ERP components (experiment 2).

## RESULTS

### Dissociating oscillatory underpinnings and behavioral correlates of the P1- and P3-evoked response

The first goal of the present study was to investigate and possibly dissociate the oscillatory underpinnings and behavioral correlates of early (C1/P1) and later (P3) visual-evoked responses. To this end, we measured in the first experiment prestimulus alpha oscillatory activity (Figure 1A) and ERPs (Figure 1B) during a visuospatial perception task in which participants were requested to provide accurate responses and confidence ratings (for details, see STAR Methods).

The first important finding is that prestimulus individual alpha frequency (IAF) negatively correlated with the latency of the P1-evoked response to the visual stimulus ($r = -0.697$, CI = [−0.799–0.573]). No relationship was found with P1 amplitude ($r = -.213$, CI = [−0.521, 0.103]). In other words, the faster the prestimulus IAF, the earlier the P1 (Figure 2A). Crucially, both prestimulus alpha frequency and latency of the P1 component seem to be closely related to task outcome. Specifically, faster alpha frequency and earlier P1 latencies were both associated with higher task accuracy, as measured via d-prime score (alpha frequency: $r = 0.408$, CI = [0.135, 0.633]; P1 latency: $r = -0.309$, CI = [−0.561, −0.024], Figures 2B and 2C). No relationship was found between task accuracy and P1 amplitude ($r = -0.092$, CI = [−0.413, 0.202). In addition, control analyses confirmed the specificity of these relations, as the IAF was neither associated with latency nor amplitude of the P3 component (P3 latency: $r = 0.104$, CI = [−0.251, 0.505]; P3 amplitude: $r = 0.220$, CI = [−0.140, 0.535]), nor was there an association of P3 with task accuracy (P3 latency: $r = 0.056$, CI = [−0.231, 0.334]; P3 amplitude: $r = 0.107$, CI = [−0.219, 0.437]).

By contrast, prestimulus alpha amplitude was closely related to the size of the subsequent P3-evoked response. Specifically, lower alpha amplitude prior to the stimulus was associated with higher P3 amplitude ($r = -0.341$, CI = [−0.575, −0.068], Figure 2A), but did not significantly correlate with the P3 latency ($r = 0.021$, CI = [−0.273, 0.295]). Furthermore, this lower alpha amplitude and the higher P3 component both predicted perceptual confidence levels (alpha amplitude: $r = -0.412$, CI = [−0.643, −0.155]; p3 amplitude: $r = 0.467$, CI = [0.175, 0.698], Figures 2B and 2C), with lower alpha/higher P3 amplitude being associated with higher confidence ratings. No relationship was observed between confidence ratings and P3 latency ($r = 0.215$, CI = [−0.056, 0.497]). Moreover, prestimulus alpha amplitude was not related to the P1-evoked response (P1 latency: $r = 0.151$,

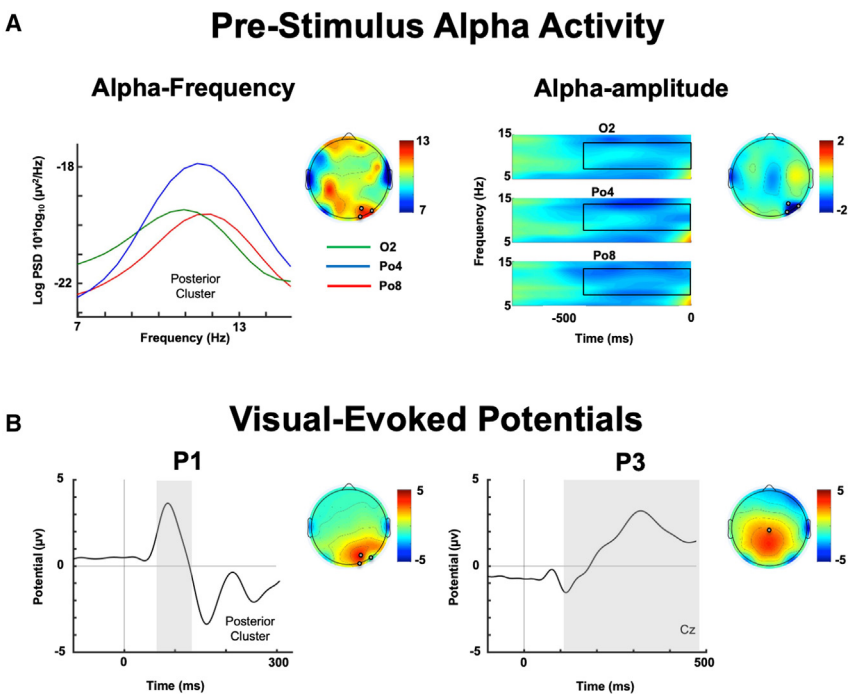


**Figure 1. Prestimulus alpha activity and visual-evoked potentials**

(A) Prestimulus Alpha activity: the left plot represents averaged alpha frequency as the mean power spectral density (PSD) (10 × log10 [mv2/Hz]) in the prestimulus time period for electrodes of the posterior cluster (Po8, Po4, and O2) contralateral to stimulus presentation. The topography represents the distribution of the individual alpha-frequency peaks. The right plot illustrates prestimulus alpha amplitude as time-frequency plots in the contralateral posterior cluster. Black boxes denote regions of statistical analyses. Topography represents the distribution of alpha amplitude (electrodes are flipped to have contralateral activity on the right-hand side and ipsilateral activity on the left-hand side).

(B) Visual-evoked potentials: grand average stimulus-locked ERP waveforms at the posterior cluster (on the left column) and at electrode Cz (on the right column). Shaded gray bars denote regions of statistical analyses (between 70 and 130 ms for the P1 and between 100 and 500 ms for the P3). Topographies represent the amplitudes of positive peaks in the P1 and P3 time windows (electrodes are flipped to have contralateral activity on the right-hand side and ipsilateral activity on the left-hand side).

See also Figures S1–S3. µv, microvolt; Hz, hertz; ms, milliseconds.

CI = [−0.091, 0.381]; P1 amplitude: r = 0.155, CI = [−0.015, 0.489]) and there was no relationship between P1-evoked responses and confidence ratings (P1 latency: r = −0.026, CI = [−0.430, 0.334]; P1 amplitude: r = −0.253, CI = [−0.473, 0.139]), thus demonstrating the specificity of the association of alpha amplitude with P3 magnitude.

Finally, analyses of C1 latencies and amplitudes were inconclusive (as the component was undetectable in some participants), although our design using checkerboard stimuli should have allowed testing C1 responses. The difficulty in detecting C1 could have arisen from us employing only stimuli appearing in the left and right lower visual field (lVF). With these types of stimuli, we can expect a positive C1 component in a somewhat earlier, but overlapping, window relative to P1. Moreover, although more central than P1, C1 components to lVF stimuli have a posterior distribution. This makes it difficult to distinguish between the C1- and P1-evoked response when using lVF stimuli only. However, a careful inspection of our data suggests that the positive peak that we detect over posterior electrodes is more likely to represent P1 and that C1 might not be visible in our data. Specifically, the positive peak that is detectable is more lateralized, stronger in the hemisphere contralateral to the stimulus location, and appearing around 90-ms after stimulus onset, which is somewhat later than when the C1 would be expected (see Figures S1 and S2).

## Causal confirmation of the double-dissociated, oscillatory underpinnings of the P1- and P3-evoked response

In experiment 1, we were able to reveal a double dissociation of oscillatory parameters of prestimulus alpha oscillations (frequency and amplitude, respectively) in respect to their electrophysiological correlates in post-stimulus-evoked responses (namely P1 and P3 components, respectively). In experiment 2, we directly manipulated these prestimulus alpha parameters to test whether they may causally underlie these subsequent evoked response component effects (namely modulations in P1 latency and P3 amplitude, respectively). To this end, we applied a 5-pulse rhTMS train of fixed intensity (60% of the maximum stimulator output) to the right occipital cortex (coil placement over O2) prior to stimulus presentation in three distinct groups of participants (IAF + 1 Hz group, IAF − 1 Hz group, IAF group) to entrain their prestimulus alpha oscillations toward a faster/slower pace, respectively (IAF ± 1 Hz groups), or to enhance alpha amplitude via entrainment (IAF group).[43] Along with active stimulation, sham stimulation at the matching frequency was also implemented for every participant to account for any non-specific effect of rhTMS. We previously reported the electrophysiological results from concurrent EEG recordings confirming the expected rhTMS outcome during the stimulation itself: rhTMS successfully slowed down/speeded up IAF online to rhTMS (prestimulus) in the IAF−1/IAF+1 group, while there was no modulation of alpha frequency in the IAF group. The broadband alpha amplitude, on the other hand, was enhanced across all of the active entrainment protocols, with the maximum entrainment effect for rhTMS at the exact stimulation frequency (IAF group).[7,44] Likewise, we previously reported behavioral outcomes of these entrainment protocols linking the changes in IAF and alpha amplitude to perceptual accuracy and confidence,[7] which were again confirmed here in experiment 1 and extended to a wider group of participants. Therefore, we here focus on the effects of the rhTMS protocols on subsequent ERPs.

Our results showed that the latency of the P1-evoked component in the two hemispheres depended on TMS relative to SHAM stimulation and the experimental group of participants (STIMULATIONxGROUP interaction, F(2,48) = 6.18; p =.004;

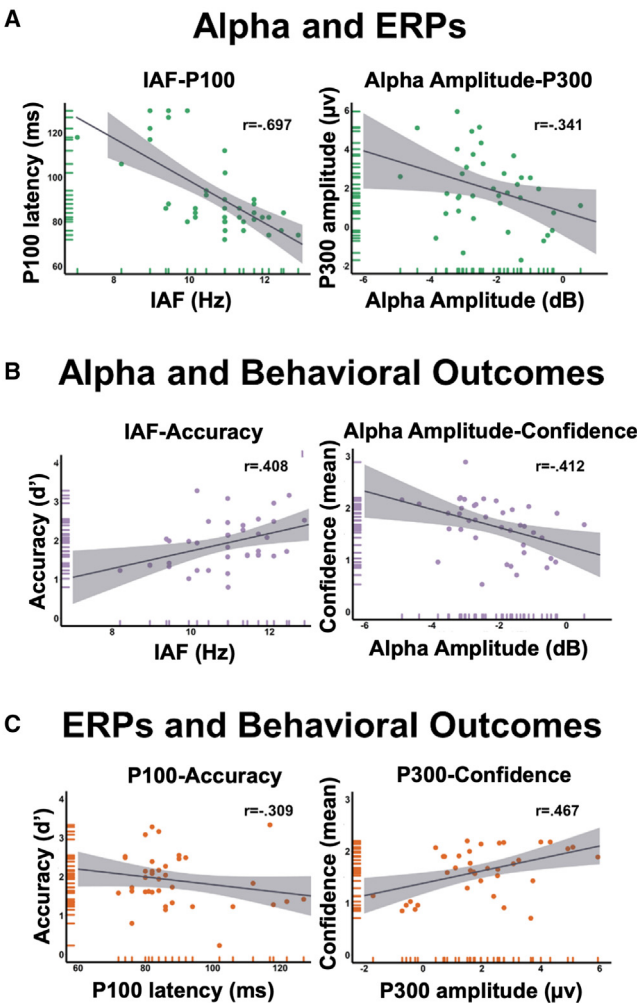


**Figure 2. Results of experiment 1: dissociating oscillatory underpinnings and behavioral correlates of the P1- and P3-evoked response**

(A) Correlation plots between prestimulus alpha activity (IAF, upper plot, and alpha amplitude, lower plot) and ERPs (P1 latency, upper plot, and P3 amplitude, lower plot). See also Figure S4.

(B) Correlation plots between prestimulus alpha activity (IAF, upper plot, and alpha amplitude, lower plot) and behavioral outcomes (accuracy, upper plot, and confidence, lower plot).

(C) Correlation plots between ERPs (P1 latency, upper plot, and P3 amplitude, lower plot) and behavioral outcomes (accuracy, upper plot, and confidence, lower plot). All correlations presented in the figure were significant, as estimated via robust Pearson skipped correlations. Gray shades around the regression line present a 95% confidence interval estimated via linear model. ms, milliseconds; Hz, hertz; mv, microvolt; dB, decibel; d′, d-prime.res.

ηp2 =.205) (Figure 3A). Further exploration of the data confirmed that speeding up the right hemisphere alpha frequency led to shorter P1 latencies during active (vs. sham) stimulation in the same (right) hemisphere ($M_{tms}$ = 77.67; $M_{sham}$ = 84.18; t(16) = 2.62, p =.019; d = 0.63) (Figure 3B). In contrast, slowing-down prestimulus alpha frequency by rhTMS led to later P1 latencies during active compared with sham stimulation in the stimulated (right) hemisphere ($M_{tms}$ = 90.23; $M_{sham}$ = 84.63; t(16) = 2.46, p =.026; d = 0.60). Furthermore, inducing higher alpha amplitude in the right hemisphere did not yield any differences in the P1 latency ($M_{tms}$ = 87.27; $M_{sham}$ = 87.23; t(16) = 0.15, p =.988; d = 0.04) (Figure 3C).

Although the above confirmed that prestimulus alpha frequency, but not alpha amplitude, has a causative role in the genesis of the P1 component, we also aimed to determine whether modulations of prestimulus alpha amplitude, which was enhanced in all groups by rhTMS (see above), in turn causally shape the amplitude of the P3 response. Indeed, we found that the P3 amplitude was modulated by rhTMS relative to sham across all three groups of participants (main effect of STIMULATION, F(2,48) = 10.22; p =.002; ηp2 =.176) (Figure 4A). The higher prestimulus alpha amplitude induced in all the groups led to lower P3 amplitude during active (vs. sham) stimulation in the stimulated hemisphere (Figure 4B). Further analyses demonstrated that the difference is only significant for the IAF group ($M_{tms}$ = 1.945; $M_{sham}$ = 2.595; t(16) = 2.37, p =.031; d = 0.57), while differences in the IAF−1 and IAF+1 groups, although going in the same direction, did not reach significance (t(16) < 1.74, p >.100; d < 0.42) (Figure 4C), in accordance with the entrainment effects on alpha amplitude, which were shown to be strongest in this group.[7]

Taken together, the present results point to a distinct role for alpha frequency and alpha amplitude in shaping evoked responses: while alpha frequency seems to directly determine the exact timing of the early P1 component, alpha amplitude selectively shapes the later P3-evoked response.

## DISCUSSION

The present findings provide novel support for the oscillatory model of ERP generation, showing that, at least in part, evoked responses are causally shaped by the ongoing oscillatory activity. Although there is increasing evidence that background EEG is, in fact, task-relevant, and various studies have repeatedly questioned the validity of the evoked model of ERP generation, arguing that ERPs originate from a reset of ongoing oscillations,[14,16–21] an actual case for phase reorganization has been proven difficult to build due to various methodological reasons.[20] By manipulating oscillatory activity via non-invasive neurostimulation protocols through online, rhythmic TMS, and examining the consequences on evoked responses, the main aim of the present study was to contribute to closing this gap between studies of brain oscillations and evoked responses. Our data causally link prestimulus brain oscillations to post-stimulus-evoked responses, and by linking specific features of ongoing alpha oscillations (namely frequency and amplitude) to specific features of early- and late-evoked responses (namely latency and magnitude) and perception, shed new light on oscillatory mechanisms of ERP genesis and their functional relevance.

### Evidence for at least two mechanisms of ERP genesis through prestimulus alpha oscillations

Our results across the two experiments unequivocally support the dependence of ERPs on prestimulus alpha activity, whereby alpha frequency and alpha amplitude shape distinct evoked components. Specifically, faster or slower prestimulus alpha activity led to earlier or later P1 latencies. By contrast, higher or lower prestimulus alpha amplitude determined lower or higher P3 amplitude, in line with previous findings[45–47] (but see Iemi et al.[48] and Studenova et al.[49] for a different account). Given

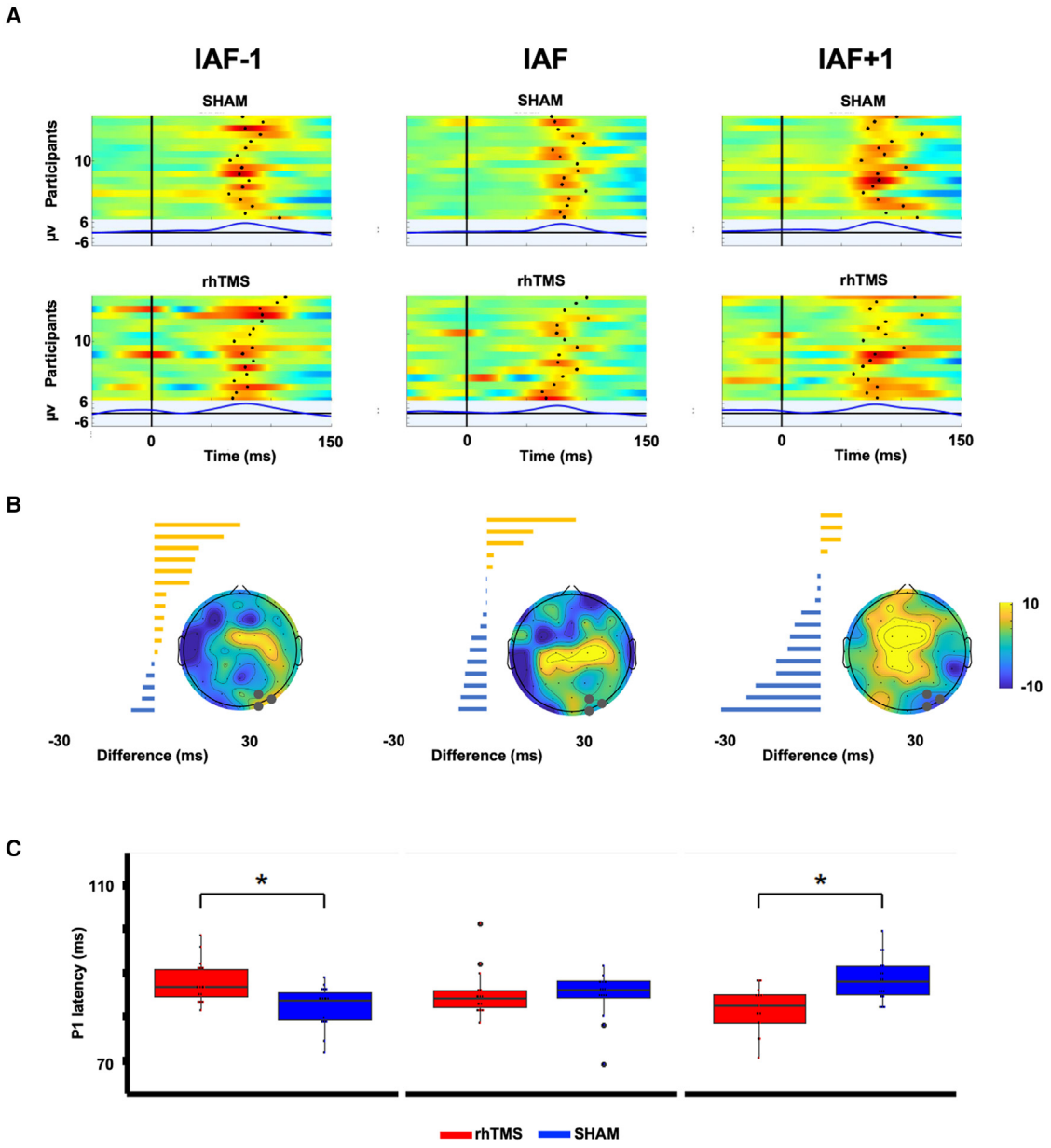


**Figure 3. Results of experiment 2: IAF shapes P1 latency**

(A) Grand ERP-image plots over the posterior electrode cluster (Po4, Po8, and O2) for SHAM (upper row), rhTMS (middle row), and the difference rhTMS-SHAM (lower row) conditions in the IAF−1 (first column), IAF (second column), and IAF+1 (third column) groups. In each plot, participants are sorted by the change rate of the latencies between the rhTMS and SHAM and single-subject P1 peak is marked with a dot. Vertical lines at 0 ms indicate stimulus onset. In the lower part of each plot, the grand averages ERPs are presented in the P100 time window (70–130 ms).

(B) Bar graphs represent the distribution of the difference in P100 peak latency between rhTMS and SHAM for each subject. Topographies represent the difference in P100 peak latency between rhTMS and SHAM for each group.

(C) Boxplots illustrate P100 latency calculated on near-stimulation posterior electrode cluster during rhTMS and SHAM for each group. Data are presented as median (full line) ± 1 quartile (box limits). The upper/lower whiskers extend to the 1.5* IQR (interquartile range). Data beyond the whiskers are plotted individually. Two-tailed t test statistical significance is reported (*$p < 0.05$). μv, microvolt; Hz, hertz; ms, milliseconds; amp, amplitude.

that the influence of prestimulus alpha oscillations on these post-stimulus responses differs in effect quality (affecting latency vs. magnitude), we conclude that the mechanisms underlying the oscillatory effects on earlier vs. later ERPs must be distinct, thus confirming the assumption that the oscillatory model of ERP genesis could manifest in more than one mechanism.[13,48]

On the one hand, the influence of IAF on P1 latency is best explained through a phase reorganization of ongoing alpha oscillations. According to the phase reset account in which phases of ongoing oscillations become aligned by the stimulus, averaging these phase-locked oscillations across trials would not result in phase cancellation in the post-stimulus window. Instead, phase

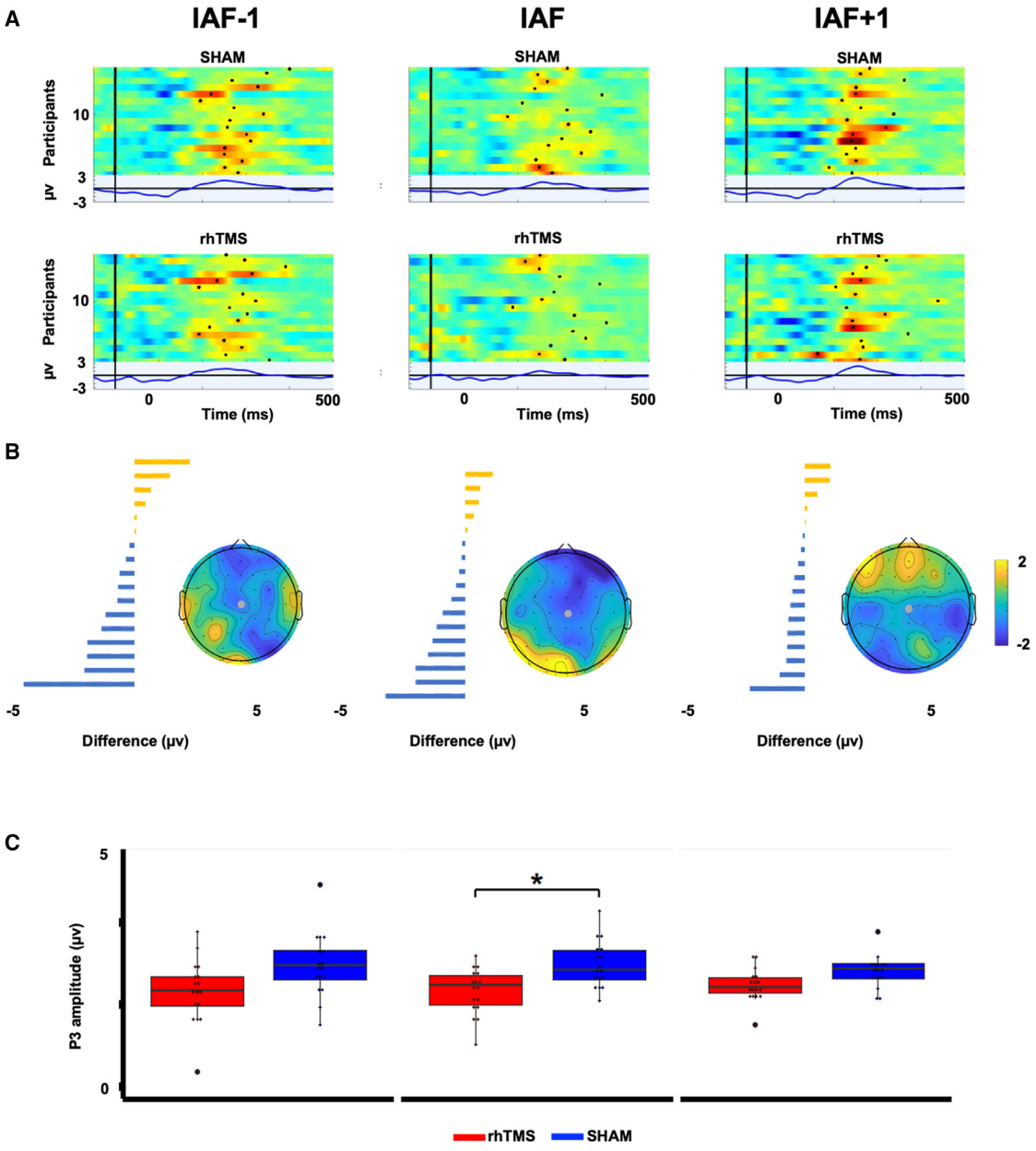


**Figure 4. Results of experiment 2: Alpha amplitude shapes P3 amplitude**

(A) Grand ERP-image plots over the electrode Cz for SHAM (upper row), rhTMS (middle row), and their difference – rhTMS-SHAM (lower row) conditions in the IAF−1 (first column), IAF (second column), and IAF+1 (third column) groups. In each plot, participants are sorted by the change rate of the amplitude between the rhTMS and SHAM, and single-subject P3 peak is marked with a dot. Vertical lines at 0 ms indicate stimulus onset. In the lower part of each plot, the grand average ERPs are presented in the P300 time window (100–500 ms).

(B) Bar graphs represent the distribution of the difference in P300 amplitude between rhTMS and SHAM for each subject. Topographies represents the difference in P300 amplitude between rhTMS and SHAM conditions for each group.

(C) Boxplots report P300 amplitude calculated on Cz during rhTMS and SHAM for each group. Data are presented as median (full line) ± 1 quartile (box limits). The upper/lower whiskers extend to the 1.5* IQR (interquartile range). Data beyond the whiskers are plotted individually. Two-tailed t test statistical significance is reported (*$p < 0.05$). μv, microvolt; Hz, hertz; ms, milliseconds; amp, amplitude.

realignment would be expected to lead to the generation of a post-stimulus component that has a similar frequency and unchanged power characteristics relative to the prestimulus oscillation.[20] The modulation of P1 by the prestimulus alpha manipulation we observed is in line with these predictions for several reasons. First, we found this early component to show the expected peak latency at the delay of one alpha cycle (~100 ms), in accordance with the phase reorganization of alpha activity in response to stimulus appearance. Second, P1 characteristics exactly mirrored the rhTMS-induced changes in prestimulus alpha frequency, with phase-reset of faster alpha frequencies expected to lead to shorter P1 peak latencies (due

to shorter prestimulus alpha cycles) and phase-reset of slower alpha frequencies expected to lead to later P1 peak latencies (due to longer prestimulus alpha cycles), hence further supporting the notion that the P1 responses were shaped by phase-reorganization of prestimulus oscillations. Third, there was no modulation of the P1 amplitude across all rhTMS-entrainment conditions, in accordance with a phase reorganization model of the P1 genesis.

On the other hand, phase-reset cannot explain the effect of increased prestimulus alpha amplitude on lower P3 amplitude components as not respecting pre- relative to post-stimulus power equivalence. In addition, as the alpha rhythm is much faster than the frequency content of the slow ERP component, this latter component cannot reflect the phase reorganization of prestimulus alpha activity. Instead, the slow P3 component, which is generated when the stimulus reaches conscious awareness, as demonstrated repeatedly,[45,47,50–52] is better explained by an additive mechanism[53–55] modulated by prestimulus alpha amplitude, presumably through a process of functional inhibition. Here, the higher prestimulus alpha amplitude would mean lower excitability of visual areas, resulting in an inhibitory effect that attenuates the amplitude of the additive post-stimulus ERP component.

It is worth noting that a recent EEG study obtained seemingly contradictory results to ours,[48] yet on other ERP components. Iemi et al.[48] reported prestimulus alpha amplitude to be negatively related to the size of early ERP components, namely of C1 and N150, and positively related to the size of later components (peaking 400–900 ms after stimulus onset). They interpreted these relationships to reflect functional inhibition and baseline shift mechanisms (BSMs), respectively. We cannot exclude the possibility of functional inhibition through prestimulus alpha activity on early ERP components other than P1, as our current task design did not yield a robust C1 nor N150 component. On the other hand, the finding of a later component that is linked to alpha activity through a BSM has been confirmed in a recent study.[49] Specifically, it was demonstrated that the P300 waveform closely matches the post-stimulus alpha amplitude decreases, along with a direct positive link between the strength of the pre- vs. post-stimulus alpha modulations and P3 amplitude. This is predicted by the BSM account of P3 generation, which posits that a state of higher prestimulus alpha amplitude would amplify the P3 response (instead of reducing it, as found here) due to stronger prestimulus oscillations leading to a stronger post-stimulus power suppression. This ultimately results in a greater amplitude of late ERPs after baseline correction, provided alpha oscillations show a non-zero mean (a prerequisite of the BSM account). Yet, other studies,[45,47] including ours, found an inverse relationship between prestimulus alpha amplitude and P3 amplitude, which favors an inhibitory account of alpha on late P3 generation. Therefore, although all of the aforementioned studies, including ours, converge on a conclusion that alpha is involved in the generation of the P300 and that the phase-reset mechanism can be ruled out as a candidate mechanism that binds them, the observation of opposite directions of alpha-P300 links across studies cannot be resolved within one account. Could this point to the presence of two distinct mechanisms that may be differently expressed depending on the task being probed and/or analysis approach being employed?

To identify potential sources of this discrepancy, we reanalyzed the data of experiment 1 in several different ways. First, we explored whether our finding of a negative link still holds if we probe this link in terms of trial-by-trial co-fluctuations of prestimulus alpha- and P300-amplitude (i.e., of within-participant as opposed to between-participant co-fluctuations). Specifically, we sorted the trials in three bins (i.e., in high, medium, and low prestimulus alpha amplitude) and compared the P3 amplitude between high and low alpha bins by paired t test (focusing on Cz, as above). Corroborating our between-participant results, we found a significantly higher P3 amplitude for low as compared with high alpha-amplitude trials ($t(40) = 2.301$, $p = .0267$, $d = .364$, $M_{high} = 3.538$, $SE = 0.413$; $M_{low} = 3.934$, $SE = 0.384$, see Figure S3). This confirms that our results are robust. Second, we reanalyzed the data from experiment 1 by using the same analysis approach as Iemi et al.,[48] reporting positive alpha-P300 links (i.e., using FFT instead of TF analysis and selecting electrode Pz instead of Cz). Notably, this replicated the results reported by Iemi et al.[48] and Studenova et al.,[49] also in our dataset. More specifically, we found a positive link between prestimulus alpha amplitude and P3 amplitude ($r = 0.181$, $CI = [0.014, 0.556]$), but this reanalyzed P3 amplitude did not show a correlation to task outcome in terms of confidence ratings ($r = -0.049$, $CI = [-0.413, 0.192]$). Accordingly, we infer that both BSM and inhibitory mechanisms may co-exist and explain alpha-P300 links, even within the same dataset, with, however, only the inhibitory link being functionally interpretable in our perceptual task context. Third, to shed light on a potential physiological explanation of these seemingly contradictory results in the same (our) dataset, despite rather minor differences in analyses approaches (TF vs. FFT) and electrode selection (Cz vs. Pz), we further explored our data by follow-up topographical correlation analyses (see Figure S4). One crucial aspect that differs between the two analysis approaches with opposite outcomes is the use of an additional single-trial baseline normalization during the TF analysis. This puts emphasis on the short-term variability of alpha changes right before the visual stimulus, while reducing long-term, sustained variability. Please note that it is these short-term alpha changes right before the stimulus that have previously been shown to be perceptually relevant[6,8,10,12,56] and that we attempted to emulate here via rh-TMS in experiment 2. Our follow-up analyses (see Figure S4) confirm that it is the additional baseline normalization that emphasizes inhibitory (negative) alpha-P300 links and minimizes the impact of sustained baseline shifts on P300, such as expected to be expressed through BSM. Based on these observations, we conclude that there are likely two alpha contributors to P300 variability: one that is based on short-term, perceptually relevant alpha changes, and another that is sustained over many trials (see, e.g., baseline shift), the contribution of which is minimized by baseline normalization within trials. Hence, these findings indicate that there are different roles of sustained vs. transient alpha-amplitude changes in shaping evoked responses, reconciling both our current and previous seemingly contradictory findings.

Taken together, we conclude that, although BSM can explain mechanistic links between some sustained alpha modulations and the later ERP component, other, task-relevant transient alpha modulations seem to shape a late potential of the P300 family via a functional inhibition mechanism, at least in our task

context. Importantly, this interpretation from the correlational results of experiment 1 is substantiated in experiment 2, demonstrating in a causal manner that enhancing alpha amplitude via TMS entrainment directly leads to lower P300 amplitude (not enhanced P300 amplitude, as would be expected from the baseline shift model). We hence conclude from these two complementary approaches that we have both correlative and causal evidence that functional inhibition is one of the mechanisms shaping the alpha-P300-perception link. Moreover, our additional analyses reconcile the apparently contradictory results of a positive relationship between alpha and P300 amplitude, which has previously been associated with BSMs, by highlighting different contributions of a sustained vs. momentary, transient modulation of prestimulus alpha amplitude.

### ERP geneses by alpha oscillations are functionally relevant

The two features of alpha oscillations investigated (and manipulated) here, along with their ERP dependents, showed distinct links to perceptual performance, indicating that these neural events reflect the activities of two independent mechanisms that serve complementary functions in visual decision making. In terms of alpha frequency, we have previously demonstrated that the speed of prestimulus alpha oscillations over occipital areas plays a crucial and selective role in modulating perceptual sensitivity, with faster vs. slower alpha frequencies leading to higher vs. lower perceptual accuracy of detecting briefly presented stimuli.[7] These results complement previous literature on the discrete sampling/perceptual framing potential of the alpha frequency, where higher frequency would translate into better temporal sensitivity/resolution, best revealed through temporal tasks. Taken together, these results demonstrate that higher alpha frequency is not only expected to aid temporal resolution by creating more sampling frames per second but, at the same time, that the higher frequency also means that less time is employed to create a single sampling frame, leading to higher processing capacities. In accordance with this framework, here we observed that inducing faster alpha oscillations was followed by an earlier P1 peak and higher perceptual accuracy. Conversely, inducing a slower alpha rhythm led to the genesis of comparatively late P1 peaks, in turn associated with lower accuracy levels. We speculate that the P1 response might represent a critical, stimulus-aligned sweep of visual sampling for efficient stimulus processing in resonance with the prestimulus alpha cycles. Prestimulus alpha amplitude, on the other hand, has been proposed to relate to internal decision-making variables that shape conservative (high-alpha-amplitude values) to liberal response criteria (low-alpha-amplitude values), rather than perceptual accuracy per se.[6–8,12] Mechanistically, prestimulus alpha-amplitude modulations have been linked to neural excitability changes that will affect both signal and noise, hence biasing the perceptual report to a more subjective (than objective) interpretations of signals (or noise).[8] It is, therefore, only to be expected that exactly these modulations of prestimulus alpha amplitude would directly influence the P3 amplitude that was selectively related to confidence levels. Being one of the most-investigated ERP components, there is abundant evidence of various functional roles of the P3 component, ranging from information processing, attentional control, and monitoring to reflecting subjective awareness.[40,41,50,57–62] Moreover, there is an ongoing debate about whether the P3 component can be modulated by visual awareness (i.e., detection of a peri-threshold stimulus) and/or subjective report and confidence, fueled by thus far contrasting results.[40,41,63–65] Our findings favor the latter view, as P3 amplitude was positively associated with confidence measures but not detection rate. Taken together, and in line with previous findings associating the P3 component with stimulus relevance,[66–68] attention,[58,69] and confidence,[63] it is reasonable to conclude that components of the P3 family reflect a mechanism that shapes our subjective interpretation of events. However, this mechanism has its origin long before the P3 is generated, as prestimulus alpha activity already dictates the level of our initial perceptual bias, shaping both subjective stimulus evaluation and neural-evoked responses reflected in P3 amplitude.

### Other considerations

Although our results indicate that prestimulus alpha activity directly influences subsequent ERP components, we acknowledge that a one-to-one linear relationship is unlikely and overly simplified. Oscillations interact constantly among themselves,[70,71] and are themselves influenced by stimulus presentation and post-stimulus processes: all processes likely to affect ERP genesis itself. Likewise, considering that not only alpha but also all EEG oscillations have a common operating principle, that is, the control of timing of neural activity,[72] it is conceivable that task-relevant oscillations will interact and consequently shape task-specific evoked components. For instance, in a memory recognition task, it is reasonable to assume that both hippocampal theta activity, known to influence memory processes and sensory encoding,[73] and alpha activity, influencing processing of sensory-semantic information,[74,75] will interact to give rise to ERPs. Yet, here we provide the first causal demonstration of a linear relationship between different parameters of alpha oscillatory activity and specific evoked components in response to a visual stimulus presentation.

### Conclusions

Our study sheds new light on the relationship between prestimulus oscillations and the genesis of functionally relevant evoked components. By establishing a causal dissociation of IAF and alpha amplitude in shaping P1 and P3 responses, this study provides fundamental evidence in favor of the oscillatory model. In contrast to previous studies that advocated for the oscillatory model based solely on EEG evidence[15,17,47,48] (or e.g., theoretical models[13]), we here unravel the inter-dependence of prestimulus oscillations and post-stimulus ERP responses through causal approaches for oscillatory entrainment. Our results confirm the notion that there are different mechanisms underlying the oscillatory model[13]: while phase reset of alpha activity can best explain the genesis of the earlier P1 component, P3 seems to be influenced by functional inhibitory mechanisms through transient modulations of task-relevant alpha oscillations in a perceptual context, alongside BSMs more related to sustained alpha modulations.

## STAR★METHODS

Detailed methods are provided in the online version of this paper and include the following:

## SUPPLEMENTAL INFORMATION

Supplemental information can be found online at https://doi.org/10.1016/j.cub.2024.01.069.

## ACKNOWLEDGMENTS

V.R. is supported by the Italian MUR – Ministry of University (P2022XAKXL and 2022H4ZRSN) and by the Ministerio de Ciencia, Innovación y Universidades (PID2019-111335GA-100).

## AUTHOR CONTRIBUTIONS

Conceived the project, V.R. and G.T.; designed the experiments, V.R., J.T., F.D.G., and G.T.; performed the experiments, J.T.; analyzed the data, J.T. and F.D.G.; wrote the paper, J.T., F.D.G., G.T., and V.R.

## DECLARATION OF INTERESTS

The authors declare no competing interests.

Received: May 26, 2023
Revised: October 6, 2023
Accepted: January 26, 2024
Published: February 19, 2024

## REFERENCES

1. Başar, E., Başar-Eroğlu, C., Karakaş, S., and Schürmann, M. (2000). Brain oscillations in perception and memory. Int. J. Psychophysiol. *35*, 95–124.
2. Jensen, O., Spaak, E., and Zumer, J.M. (2019). Human Brain Oscillations: From Physiological Mechanisms to Analysis and Cognition. In Magnetoencephalography: From Signals to Dynamic Cortical Networks, S. Supek, and C.J. Aine, eds. (Springer International Publishing), pp. 471–517.
3. Mazaheri, A., Slagter, H.A., Thut, G., and Foxe, J.J. (2018). Orchestration of brain oscillations: Principles and functions. Eur. J. Neurosci. *48*, 2385–2388.
4. Palva, S., and Palva, J.M. (2007). New vistas for alpha-frequency band oscillations. Trends Neurosci. *30*, 150–158.
5. Ward, L.M. (2003). Synchronous neural oscillations and cognitive processes. Trends Cogn. Sci. *7*, 553–559.
6. Benwell, C.S.Y., Tagliabue, C.F., Veniero, D., Cecere, R., Savazzi, S., and Thut, G. (2017). Prestimulus EEG Power Predicts Conscious Awareness But Not Objective Visual Performance. eNeuro *4*, 182–17.2017. eNeuro.
7. Di Gregorio, F., Trajkovic, J., Roperti, C., Marcantoni, E., Di Luzio, P., Avenanti, A., Thut, G., and Romei, V. (2022). Tuning alpha rhythms to shape conscious visual perception. Curr. Biol. *32*, 988–998.e6.
8. Iemi, L., Chaumon, M., Crouzet, S.M., and Busch, N.A. (2017). Spontaneous Neural Oscillations Bias Perception by Modulating Baseline Excitability. J. Neurosci. *37*, 807–819.
9. Limbach, K., and Corballis, P.M. (2016). Prestimulus alpha power influences response criterion in a detection task. Psychophysiology *53*, 1154–1164.
10. Romei, V., Brodbeck, V., Michel, C., Amedi, A., Pascual-Leone, A., and Thut, G. (2008). Spontaneous fluctuations in posterior alpha-band EEG activity reflect variability in excitability of human visual areas. Cereb. Cortex *18*, 2010–2018.
11. Romei, V., Gross, J., and Thut, G. (2010). On the Role of Prestimulus Alpha Rhythms over Occipito-Parietal Areas in Visual Input Regulation: Correlation or Causation? J. Neurosci. *30*, 8692–8697.
12. Samaha, J., Iemi, L., and Postle, B.R. (2017). Prestimulus alpha-band power biases visual discrimination confidence, but not accuracy. Conscious. Cogn. *54*, 47–55.
13. Klimesch, W., Sauseng, P., Hanslmayr, S., Gruber, W., and Freunberger, R. (2007). Event-related phase reorganization may explain evoked neural dynamics. Neurosci. Biobehav. Rev. *31*, 1003–1016.
14. Klimesch, W., Schack, B., Schabus, M., Doppelmayr, M., Gruber, W., and Sauseng, P. (2004). Phase-locked alpha and theta oscillations generate the P1-N1 complex and are related to memory performance. Brain Res. Cogn. Brain Res. *19*, 302–316.
15. Mazaheri, A., and Jensen, O. (2010). Rhythmic Pulsing: Linking Ongoing Brain Activity with Evoked Responses. Front. Hum. Neurosci. *4*, 177.
16. Fuentemilla, L., Marco-Pallarés, J., and Grau, C. (2006). Modulation of spectral power and of phase resetting of EEG contributes differentially to the generation of auditory event-related potentials. NeuroImage *30*, 909–916.
17. Gruber, W.R., Klimesch, W., Sauseng, P., and Doppelmayr, M. (2005). Alpha phase synchronization predicts P1 and N1 latency and amplitude size. Cereb. Cortex *15*, 371–377.
18. Hanslmayr, S., Klimesch, W., Sauseng, P., Gruber, W., Doppelmayr, M., Freunberger, R., Pecherstorfer, T., and Birbaumer, N. (2007). Alpha phase reset contributes to the generation of ERPs. Cereb. Cortex *17*, 1–8.
19. Makeig, S., Westerfield, M., Jung, T.P., Enghoff, S., Townsend, J., Courchesne, E., and Sejnowski, T.J. (2002). Dynamic Brain Sources of Visual Evoked Responses. Science *295*, 690–694.
20. Sauseng, P., Klimesch, W., Gruber, W.R., Hanslmayr, S., Freunberger, R., and Doppelmayr, M. (2007). Are event-related potential components generated by phase resetting of brain oscillations? A critical discussion. Neuroscience *146*, 1435–1444.
21. Sayers, B.McA., Beagley, H.A., and Henshall, W.R. (1974). The mechanism of auditory evoked EEG responses. Nature *247*, 481–483.
22. Cooke, J., Poch, C., Gillmeister, H., Costantini, M., and Romei, V. (2019). Oscillatory Properties of Functional Connections Between Sensory Areas Mediate Cross-Modal Illusory Perception. J. Neurosci. *39*, 5711–5718.
23. Di Gregorio, F., Petrone, V., Casanova, E., Lullini, G., Romei, V., Piperno, R., and La Porta, F. (2023). Hierarchical psychophysiological pathways subtend perceptual asymmetries in Neglect. NeuroImage *270*, 119942.
24. Migliorati, D., Zappasodi, F., Perrucci, M.G., Donno, B., Northoff, G., Romei, V., and Costantini, M. (2020). Individual Alpha Frequency Predicts Perceived Visuotactile Simultaneity. J. Cogn. Neurosci. *32*, 1–11.
25. Pietrelli, M., Zanon, M., Làdavas, E., Grasso, P.A., Romei, V., and Bertini, C. (2019). Posterior brain lesions selectively alter alpha oscillatory activity and predict visual performance in hemianopic patients. Cortex *121*, 347–361.
26. Bertaccini, R., Ellena, G., Macedo-Pascual, J., Carusi, F., Trajkovic, J., Poch, C., and Romei, V. (2022). Parietal Alpha Oscillatory Peak Frequency Mediates the Effect of Practice on Visuospatial Working Memory Performance. Vision (Basel) *6*, 30.
27. Coldea, A., Veniero, D., Morand, S., Trajkovic, J., Romei, V., Harvey, M., and Thut, G. (2022). Effects of Rhythmic Transcranial Magnetic Stimulation in the Alpha-Band on Visual Perception Depend on Deviation

From Alpha-Peak Frequency: Faster Relative Transcranial Magnetic Stimulation Alpha-Pace Improves Performance. Front. Neurosci. *16*, 886342.

28. Tarasi, L., di Pellegrino, G., and Romei, V. (2022). Are you an empiricist or a believer? Neural signatures of predictive strategies in humans. Prog. Neurobiol. *219*, 102367.
29. Trajkovic, J., Di Gregorio, F.D., Avenanti, A., Thut, G., and Romei, V. (2023). Two oscillatory correlates of attention control in the alpha-band with distinct consequences on perceptual gain and metacognition. J. Neurosci. *43*, 3548–3556.
30. Dugué, L., Marque, P., and VanRullen, R. (2011). The Phase of Ongoing Oscillations Mediates the Causal Relation between Brain Excitation and Visual Perception. J. Neurosci. *31*, 11889–11893.
31. Samaha, J., Gosseries, O., and Postle, B.R. (2017). Distinct Oscillatory Frequencies Underlie Excitability of Human Occipital and Parietal Cortex. J. Neurosci. *37*, 2824–2833.
32. Jensen, O., and Mazaheri, A. (2010). Shaping Functional Architecture by Oscillatory Alpha Activity: Gating by Inhibition. Front. Hum. Neurosci. *4*, 186.
33. Mathewson, K.E., Lleras, A., Beck, D.M., Fabiani, M., Ro, T., and Gratton, G. (2011). Pulsed Out of Awareness: EEG Alpha Oscillations Represent a Pulsed-Inhibition of Ongoing Cortical Processing. Front. Psychol. *2*, 99.
34. Busch, N.A., and VanRullen, R. (2010). Spontaneous EEG oscillations reveal periodic sampling of visual attention. Proc. Natl. Acad. Sci. USA *107*, 16048–16053.
35. Cecere, R., Rees, G., and Romei, V. (2015). Individual differences in alpha frequency drive crossmodal illusory perception. Curr. Biol. *25*, 231–235.
36. Minami, S., and Amano, K. (2017). Illusory Jitter Perceived at the Frequency of Alpha Oscillations. Curr. Biol. *27*, 2344–2351.e4.
37. VanRullen, R. (2016). Perceptual Cycles. Trends Cogn. Sci. *20*, 723–735.
38. Di Russo, F., Martínez, A., Sereno, M.I., Pitzalis, S., and Hillyard, S.A. (2002). Cortical sources of the early components of the visual evoked potential. Hum. Brain Mapp. *15*, 95–111.
39. O'Connell, R.G., Dockree, P.M., and Kelly, S.P. (2012). A supramodal accumulation-to-bound signal that determines perceptual decisions in humans. Nat. Neurosci. *15*, 1729–1735.
40. Lamy, D., Salti, M., and Bar-Haim, Y. (2009). Neural correlates of subjective awareness and unconscious processing: an ERP study. J. Cogn. Neurosci. *21*, 1435–1446.
41. Salti, M., Bar-Haim, Y., and Lamy, D. (2012). The P3 component of the ERP reflects conscious perception, not confidence. Conscious. Cogn. *21*, 961–968.
42. Tagliabue, C.F., Veniero, D., Benwell, C.S.Y., Cecere, R., Savazzi, S., and Thut, G. (2019). The EEG signature of sensory evidence accumulation during decision formation closely tracks subjective perceptual experience. Sci. Rep. *9*, 4949.
43. Thut, G., Veniero, D., Romei, V., Miniussi, C., Schyns, P., and Gross, J. (2011). Rhythmic TMS Causes Local Entrainment of Natural Oscillatory Signatures. Curr. Biol. *21*, 1176–1185.
44. Trajkovic, J., Di Gregorio, F., Marcantoni, E., Thut, G., and Romei, V. (2022). A TMS/EEG protocol for the causal assessment of the functions of the oscillatory brain rhythms in perceptual and cognitive processes. Star Protoc. *3*, 101435.
45. Ergenoglu, T., Demiralp, T., Bayraktaroglu, Z., Ergen, M., Beydagi, H., and Uresin, Y. (2004). Alpha rhythm of the EEG modulates visual detection performance in humans. Brain Res. Cogn. Brain Res. *20*, 376–383.
46. Vigué-Guix, I., and Soto-Faraco, S. (2022). Using occipital α-bursts to modulate behaviour in real-time. bioRxiv. https://doi.org/10.1101/2022.09.21.508882.
47. Zazio, A., Ruhnau, P., Weisz, N., and Wutz, A. (2022). Pre-stimulus alpha-band power and phase fluctuations originate from different neural sources and exert distinct impact on stimulus-evoked responses. Eur. J. Neurosci. *55*, 3178–3190.
48. Iemi, L., Busch, N.A., Laudini, A., Haegens, S., Samaha, J., Villringer, A., and Nikulin, V.V. (2019). Multiple mechanisms link prestimulus neural oscillations to sensory responses. eLife *8*, e43620.
49. Studenova, A., Forster, C., Engemann, D.A., Hensch, T., Sanders, C., Mauche, N., Hegerl, U., Loffler, M., Villringer, A., and Nikulin, V.V. (2023). Event-related modulation of alpha rhythm explains the auditory P300-evoked response in EEG. eLife *12*, RP88367.
50. Dehaene, S., and Changeux, J.P. (2011). Experimental and Theoretical Approaches to Conscious Processing. Neuron *70*, 200–227.
51. Min, B.K., and Herrmann, C.S. (2007). Prestimulus EEG alpha activity reflects prestimulus top-down processing. Neurosci. Lett. *422*, 131–135.
52. Sanchez, G., Hartmann, T., Fuscà, M., Demarchi, G., and Weisz, N. (2020). Decoding across sensory modalities reveals common supramodal signatures of conscious perception. Proc. Natl. Acad. Sci. USA *117*, 7437–7446.
53. Mazaheri, A., and Jensen, O. (2006). Posterior α activity is not phase-reset by visual stimuli. Proc. Natl. Acad. Sci. USA *103*, 2948–2952.
54. Shah, A.S., Bressler, S.L., Knuth, K.H., Ding, M., Mehta, A.D., Ulbert, I., and Schroeder, C.E. (2004). Neural Dynamics and the Fundamental Mechanisms of Event-related Brain Potentials. Cereb. Cortex *14*, 476–483.
55. Haegens, S., Nácher, V., Luna, R., Romo, R., and Jensen, O. (2011). α-Oscillations in the monkey sensorimotor network influence discrimination performance by rhythmical inhibition of neuronal spiking. Proc. Natl. Acad. Sci. USA *108*, 19377–19382.
56. Samaha, J., Iemi, L., Haegens, S., and Busch, N.A. (2020). Spontaneous Brain Oscillations and Perceptual Decision-Making. Trends Cogn. Sci. *24*, 639–653.
57. Förster, J., Koivisto, M., and Revonsuo, A. (2020). ERP and MEG correlates of visual consciousness: The second decade. Conscious. Cogn. *80*, 102917.
58. Koivisto, M., Revonsuo, A., and Lehtonen, M. (2006). Independence of Visual Awareness from the Scope of Attention: An Electrophysiological Study. Cereb. Cortex *16*, 415–424.
59. Polich, J. (2007). Updating P300: an integrative theory of P3a and P3b. Clin. Neurophysiol. *118*, 2128–2148.
60. Rutiku, R., Martin, M., Bachmann, T., and Aru, J. (2015). Does the P300 reflect conscious perception or its consequences? Neuroscience *298*, 180–189.
61. Verleger, R., Jaśkowski, P., and Wascher, E. (2005). Evidence for an Integrative Role of P3b in Linking Reaction to Perception. J. Psychophysiol. *19*, 165–181.
62. Volpe, U., Mucci, A., Bucci, P., Merlotti, E., Galderisi, S., and Maj, M. (2007). The cortical generators of P3a and P3b: a LORETA study. Brain Res. Bull. *73*, 220–230.
63. Eimer, M., and Mazza, V. (2005). Electrophysiological correlates of change detection. Psychophysiology *42*, 328–342.
64. Pitts, M.A., Metzler, S., and Hillyard, S.A. (2014). Isolating neural correlates of conscious perception from neural correlates of reporting one's perception. Front. Psychol. *5*, 1078.
65. Ye, M., Lyu, Y., Sclodnick, B., and Sun, H.J. (2019). The P3 Reflects Awareness and Can Be Modulated by Confidence. Front. Neurosci. *13*, 510.
66. Pitts, M.A., Martínez, A., and Hillyard, S.A. (2012). Visual processing of contour patterns under conditions of inattentional blindness. J. Cogn. Neurosci. *24*, 287–303.
67. Schelonka, K., Graulty, C., Canseco-Gonzalez, E., and Pitts, M.A. (2017). ERP signatures of conscious and unconscious word and letter perception in an inattentional blindness paradigm. Conscious. Cogn. *54*, 56–71.
68. Shafto, J.P., and Pitts, M.A. (2015). Neural Signatures of Conscious Face Perception in an Inattentional Blindness Paradigm. J. Neurosci. *35*, 10940–10948.

69. Koivisto, M., and Revonsuo, A. (2008). The role of selective attention in visual awareness of stimulus features: electrophysiological studies. Cogn. Affect. Behav. Neurosci. *8*, 195–210.

70. Fries, P. (2005). A mechanism for cognitive dynamics: neuronal communication through neuronal coherence. Trends Cogn. Sci. *9*, 474–480.

71. Palva, S., and Palva, J.M. (2012). Discovering oscillatory interaction networks with M/EEG: challenges and breakthroughs. Trends Cogn. Sci. *16*, 219–230.

72. Cohen, M.X. (2011). It's about Time. Front. Hum. Neurosci. *5*, 2.

73. Herweg, N.A., Solomon, E.A., and Kahana, M.J. (2020). Theta oscillations in human memory. Trends Cogn. Sci. *24*, 208–227.

74. Klimesch, W. (1997). EEG-alpha rhythms and memory processes. Int. J. Psychophysiol. *26*, 319–340.

75. Klimesch, W. (1999). EEG alpha and theta oscillations reflect cognitive and memory performance: a review and analysis. Brain Res. Brain Res. Rev. *29*, 169–195.

76. De Martino, B., Fleming, S.M., Garrett, N., and Dolan, R.J. (2013). Confidence in value-based choice. Nat. Neurosci. *16*, 105–110.

77. Rossi, S., Hallett, M., Rossini, P.M., and Pascual-Leone, A. (2011). Screening questionnaire before TMS: an update. Clin. Neurophysiol. *122*, 1686.

78. Rossi, S., Antal, A., Bestmann, S., Bikson, M., Brewer, C., Brockmöller, J., Carpenter, L.L., Cincotta, M., Chen, R., Daskalakis, J.D., et al. (2021). Safety and recommendations for TMS use in healthy subjects and patient populations, with updates on training, ethical and regulatory issues: Expert Guidelines. Clin. Neurophysiol. *132*, 269–306.

79. Mevorach, C., Humphreys, G.W., and Shalev, L. (2006). Opposite biases in salience-based selection for the left and right posterior parietal cortex. Nat. Neurosci. *9*, 740–742.

80. Romei, V., Thut, G., Mok, R.M., Schyns, P.G., and Driver, J. (2012). Causal implication by rhythmic transcranial magnetic stimulation of alpha frequency in feature-based local vs. global attention. Eur. J. Neurosci. *35*, 968–974.

81. Bolognini, N., Senna, I., Maravita, A., Pascual-Leone, A., and Merabet, L.B. (2010). Auditory enhancement of visual phosphene perception: the effect of temporal and spatial factors and of stimulus intensity. Neurosci. Lett. *477*, 109–114.

82. Gerwig, M., Kastrup, O., Meyer, B.U., and Niehaus, L. (2003). Evaluation of cortical excitability by motor and phosphene thresholds in transcranial magnetic stimulation. J. Neurol. Sci. *215*, 75–78.

83. Romei, V., Murray, M.M., Merabet, L.B., and Thut, G. (2007). Occipital transcranial magnetic stimulation has opposing effects on visual and auditory stimulus detection: Implications for multisensory interactions. J. Neurosci. *27*, 11465–11472.

84. Romei, V., Murray, M.M., Cappe, C., and Thut, G. (2009). Preperceptual and Stimulus-Selective Enhancement of Low-Level Human Visual Cortex Excitability by Sounds. Curr. Biol. *19*, 1799–1805.

85. Romei, V., Rihs, T., Brodbeck, V., and Thut, G. (2008). Resting electroencephalogram alpha-power over posterior sites indexes baseline visual cortex excitability. NeuroReport *19*, 203–208.

86. Delorme, A., and Makeig, S. (2004). EEGLAB: An open source toolbox for analysis of single-trial EEG dynamics including independent component analysis. J. Neurosci. Methods *134*, 9–21.

87. Gratton, G., Coles, M.G.H., and Donchin, E. (1983). A new method for off-line removal of ocular artifact. Electroencephalogr. Clin. Neurophysiol. *55*, 468–484.

88. Di Gregorio, F., Ernst, B., and Steinhauser, M. (2019). Differential effects of instructed and objective feedback reliability on feedback-related brain activity. Psychophysiology *56*, e13399.

89. Sannita, W.G., Bandini, F., Beelke, M., De Carli, F., Carozzo, S., Gesino, D., Mazzella, L., Ogliastro, C., and Narici, L. (2001). Time dynamics of stimulus- and event-related gamma band activity: contrast-VEPs and the visual P300 in man. Clin. Neurophysiol. *112*, 2241–2249.

90. Yordanova, J., and Kolev, V. (1998). Event-related alpha oscillations are functionally associated with P300 during information processing. NeuroReport *9*, 3159–3164.

91. Pernet, C.R., Wilcox, R., and Rousselet, G.A. (2012). Robust Correlation Analyses: False Positive and Power Validation Using a New Open Source Matlab Toolbox. Front. Psychol. *3*, 606.

92. Veniero, D., Bortoletto, M., and Miniussi, C. (2009). TMS-EEG co-registration: On TMS-induced artifact. Clin. Neurophysiol. *120*, 1392–1399.

93. Rogasch, N.C., Sullivan, C., Thomson, R.H., Rose, N.S., Bailey, N.W., Fitzgerald, P.B., Farzan, F., and Hernandez-Pavon, J.C. (2017). Analysing concurrent transcranial magnetic stimulation and electroencephalographic data: A review and introduction to the open-source TESA software. NeuroImage *147*, 934–951.

## STAR★METHODS

### KEY RESOURCES TABLE

| REAGENT or RESOURCE | SOURCE | IDENTIFIER |
|---|---|---|
| Deposited data | | |
| Data for all experiments reported in this paper | This paper | https://osf.io/4qxb8/ |
| Software and algorithms | | |
| RStudio v1.2.5019 | RStudio, Inc. | RRID: SCR_000432 |
| MATLAB, v. R2023b | Mathworks | RRID: SCR_001622 |
| SPSS, v23 | StatSoft, Inc. | RRID: SCR_019096 |
| Hierarchical meta-d' model (HMeta-d) | https://doi.org/10.1093/nc/nix007 | https://github.com/metacoglab/HMeta-d |
| TESA v1.1.1 toolbox | https://doi.org/10.1016/j.neuroimage.2016.10.031 | https://nigelrogasch.github.io/TESA/ |
| EEGLAB v2023.0. toolbox | https://doi.org/10.1016/j.jneumeth.2003.10.009 | RRID: SCR_007292 |
| E-prime Software | Psychology Software Tools, Inc. | RRID: SCR_009567 |
| Other | | |
| Brain Vision recorder software | Brain Products | https://brainvision.com/ |
| Magstim Rapid Transcranial Magnetic Stimulator | Magstim Company | https://www.magstim.com/ |

### RESOURCE AVAILABILITY

#### Lead contact

Further information and requests for resources should be directed to and will be fulfilled by the lead contact, Vincenzo Romei (vincenzo.romei@unibo.it).

#### Materials availability

This study did not generate new unique reagents.

#### Data and code availability

All data reported in this paper have been made publicly available through the Open Science Framework: https://osf.io/4qxb8/. Any additional information required to reanalyze the data reported in this paper is available from the lead contact upon request.

### EXPERIMENTAL MODEL AND SUBJECT DETAILS

#### Experiment 1

##### *Participants*

Forty-one healthy volunteers with normal or corrected vision participated in Experiment 1 (23 females; mean age ± SE = 23.31 ± 1.66 years). All participants were recruited at the Centre for Studies and Research in Cognitive Neuroscience in Cesena, Italy. The study was conducted in accordance with the Declaration of Helsinki and approved by the bioethics committee of the University of Bologna. All participants gave written informed consent to participate in the study.

#### Experiment 2

Please note that the experimental procedure (participants and experimental task) is the same as in Di Gregorio et al.[7] However, here the focus of analysis is on the post-stimulus ERPs, rather than behavior or prestimulus oscillatory activity, whose results are reported in Di Gregorio et al.[7]

##### *Participants*

Fifty-one healthy volunteers (25 females, 26 males; mean age ± SE = 23.39 ± 0.37 years) took part in Experiment 2. All of them had a normal or corrected-to-normal vision and met TMS safety criteria by self-report. All participants gave written informed consent before taking part in the study, which was conducted in accordance with the Declaration of Helsinki and approved by the local ethics committee. Here, subjects were randomly assigned to one of three groups with distinct stimulation protocols (see next paragraph for details): IAF-1Hz (group 1 = mean age 22.64 ± 0.53, nine females), IAF (group 2 = mean age 23.88 ± 0.57, eight females) and IAF+1Hz (group 3 = mean age 23.88 ± 0.77, eight females), each containing 17 participants.

## METHOD DETAILS

### Experiment 1

#### *Stimuli and task procedure*

Participants were comfortably seated in front of a CRT monitor (100 Hz refresh rate) at a viewing distance of 57 cm. E-Prime software (Psychology Software Tools, Inc., USA) was used to run the task and register responses. During the main experimental procedure, each trial consisted of a *primary visual detection task*, where participants had to respond to a peri-threshold target stimulus, and a *secondary confidence task*, in which participants rated the level of confidence in their perception on a scale 1 to 4, (ranging from 1 = no confidence at all to 4 = high confidence). Every trial started with a central fixation cross (visual angle = 0.8°). After 2000 ms, a preparatory cue (X) would replace the fixation cross, created by rotating the fixation cross by 45 degrees, lasting between 2000ms and 3000ms. After the cue, the primary task stimulus would appear at 4.1°/3.7° eccentricity (horizontal/vertical) with equal probability on the lower part of the right or left visual field (RVF or LVF) for 60 ms. The primary task stimulus could be a catch or target stimulus. Catch stimuli consisted of 8x8 black and white checkerboards (height = 4 cm; width= 4 cm. visual angle = 15.9°). Target stimuli consisted of the same checkerboard containing iso-luminant grey circles, which contrasted the black and white parts of the checkerboard. Participants were instructed to press the button (spacebar on the keyboard) whenever they would detect the peri-threshold circles embedded in the checkerboard. Response time limit was 2000ms. After the primary response, confidence ratings were collected. The Italian version of the question: "How confident are you about your percept?" was presented until participants rated their confidence, reflecting a participant's level of subjective certainty in having correctly perceived the stimulus.[76] After the confidence rating, a new trial would start. The main task consisted of five blocks with 60 trials per block (total trial number = 300) and lasted an average of 90 min. Data are part of a larger dataset where also informative cue trials were collected (not reported here).

#### *Titration session*

A titration session was run before the main experimental session to set stimuli contrast ratios corresponding to each individual's 50% perceptual threshold.[7,44] Briefly, iso-luminant circles of 8 different contrast ratios (RGB contrasts on black/white background: 28/227, 32/223, 36/219, 40/215, 44/211, 48/207 and 100/155) were presented along with catch trials (checkerboards without iso-luminant circles). Additionally, we accounted for the possible individual bias in response to catch trials by also considering the false alarm rate, along with target stimuli of different contrast for the calculation of the sigmoid function. For each iso-luminant contrast, individual performance was then entered for the calculation of the sigmoid function, in order to return the threshold value, which was subsequently used for stimuli presentation during the main task:

$$y = \frac{100}{1+e^{-\frac{x-c}{d}}}$$

Where x is the contrast value, c is the inflection point of the curve, and d is the slope of the sigmoid.

### Experiment 2

#### *Stimuli and task procedure*

Stimuli and tasks in Experiment 2 were the same as those described for Experiment 1, with the main difference being the active manipulation of alpha activity via an entrainment protocol.

Entrainment of the intrinsic oscillatory alpha activity was achieved using Rhythmic Transcranial Magnetic Stimulation (rhTMS). Specifically, prestimulus alpha activity was fine-tuned relative to individual alpha frequency using five-pulse rhTMS bursts in which the time lag between pulses was manipulated depending on the group.[7,44] Therefore, by adjusting the timing between pulses based on individual natural rhythms, we selectively manipulate the amplitude or the speed of brain rhythms. More specifically, to induce changes in the oscillatory-frequency cycle length, we applied rhTMS at a 1 Hz slower or faster pace relative to a participant's individual oscillatory frequency (IAF-1 Hz group and IAF+1 Hz group). To selectively modulate oscillatory-amplitude, the frequency of the rhTMS pulse trains was exactly matched to the intrinsic individual oscillatory-frequency of the participant, thus enhancing the synchronization of neural firing and phase alignment without influencing the speed of oscillatory activity (IAF group). The rhTMS design was in line with current safety guidelines.[77,78] For the EEG analysis of the entrainment effects, please consult our previous article, and Figure S4.

Stimulation was applied using a Magstim Rapid Transcranial Magnetic Stimulator via a 70 mm figure-of-eight coil (Magstim Company, UK), onto the right occipital site (in correspondence with O2 electrode), with the coil surface oriented tangentially to the scalp. Moreover, pulse intensity was kept fixed at 60% of the maximum stimulator output (MSO),[79,80] roughly corresponding to previously reported phosphene thresholds.[81–85] Non-specific rhTMS effects were accounted for via a within-subject sham control stimulation, obtained by a modified coil providing enough distance from the scalp (by adding a styrofoam cube to the coil itself) that would ensure the absence of an actual stimulation while maintaining coil position and tactile and acoustic sensations. Each participant underwent three consecutive rhTMS and sham blocks (a total of 900 active rhTMS pulses in a randomized order. Taken together, the experimental session included six blocks with 60 trials per block (N trials = 360). Short breaks were made between each block, making the overall task duration ~50 minutes.

#### *Titration session*

Titration was run as for Experiment 1, and as reported in our previous work.[7,29,44] Additionally, in Experiment 2, during the titration session, individual alpha peak frequency (defined as the maximum local power in the alpha frequency range) was determined in order

to calibrate rhTMS frequency. To this aim, a three-minute eyes-closed and eyes-opened resting-state EEG was recorded from 8 Ag/AgCl parieto-occipital electrodes (O1, P3, PO3, PO7; O2, P4, PO4, PO8). Individual alpha frequency peak was calculated from the power spectra of the eyes open condition, applying a fast Fourier transformation. In line with Experiment 1 (showing a local alpha power maxima over O2) and previous studies, alpha-frequency was calculated from the O2 electrode,[35,83] over which rhTMS was subsequently applied.

## QUANTIFICATION AND STATISTICAL ANALYSIS

### Experiment 1

#### *Psychophysiological recording – paradigm and acquisition*

EEG data were collected during the task from 64 Ag/AgCl electrodes (Fp1, Fp2, AF3, AF4, AF7, AF8, F1, F2, F3, F4, F7, F8, FC1, FC2, FC3, FC4, FC5, FC6, FT7, FT8, C1, C2, C3, C4, C5, C6, T7, T8, CP1, CP2, CP3, CP4, CP5, CP6, TP7, TP8, P1, P2, P3, P4, P5, P6, P7, P8, PO3, PO4, PO7, PO8, O1, O2, Fpz, AFz, Fz, FCz, Cz, CPz, Pz, POz, Oz) and from the right mastoid with Brain Vision recorder software (Brain Products, Munich, Germany). Ground electrode was placed on the right cheek, while the left mastoid served as online reference. The electrooculogram (EOG) was recorded from above and below the left eye and from the outer canthi of both eyes. During the recording, a band-pass filter of 0.01–100 Hz was used, along with a sampling rate of 1000 Hz. The impedance of all electrodes was kept below ten kΩ. EEG data were pre-processed using custom made routines in MatLab R2013b (The Mathworks, Natick, MA, USA). EEG data were re-referenced offline to the average of all electrodes and filtered with a 0.5–30 Hz pass-band. After applying a filter, stimulus-locked epochs were extracted (from -1500 ms to 2500 ms after stimulus presentation). Artifact-contaminated trials were excluded via pop_autorej function in EEGLAB v13.0.1,[86] which excludes high-voltage (fluctuations larger than 1000 μV) and trials identified as outliers (trials with data values outside 5 SD). Subsequently, artifacts related to eye movement were corrected via a procedure based on a linear regression method (lms_regression function in MatLab R2013b).[87] Because perceptually relevant, prestimulus alpha activity shows hemispheric lateralization relative to upcoming stimulus location, we thus recoded electrode positions as contralateral versus ipsilateral to the hemifield of stimulus presentation (resulting in all contralateral activity being on one side, which was conventionally defined to be the right), i.e., for RVF-stimulus epochs, data from the contralateral (left) electrodes were copied and flipped to right-sided electrodes.

#### *Psychophysiological recording – EEG analyses*

Alpha oscillations (frequency and amplitude) were analyzed in a prestimulus time window between -400 ms and stimulus presentation in a cluster of contralateral and ipsilateral parieto-occipital electrodes (O1, O2, Po3, Po4, Po7, Po8).

In order to identify the alpha-frequency peaks during the task, a fast Fourier transformation (MatLab function spectopo, frequency resolution: 0.166Hz) was applied. Power was calculated separately for each subject and condition and was normalized by z-score decibel ($dB = 10*\log_{10}$[-power/baseline]) transformation at each frequency. Individual alpha-frequency was defined within the contralateral cluster as the local maximum power in the electrode with the largest power within the frequency range 7–13Hz (i.e., alpha peak).[7,44]

The amplitude of alpha oscillations was calculated by time-frequency analyses of data epoched from 2000ms before to 2000ms after the stimulus onset. Long epochs prevent edge artifacts from contaminating time-frequency power in the time windows of interest. Spectral EEG activity was assessed by time-frequency decomposition using a complex sinusoidal wavelet convolution procedure (between 2 and 25 cycles per wavelet, linearly increasing across 50 linear-spaced frequencies from 2.0Hz to 50.0Hz) with the newtimef function from EEGLAB v13.0.186 and custom routines in MatLab. The resulting power was normalized by decibel ($dB = 10*\log_{10}$[-power/baseline]) transformation at each frequency, using a single trial baseline between -1000 and -500 preceding stimulus onset. This long baseline window was used to increase the signal-to-noise ratio during the baseline period and is frequently applied in time frequency analyses.[44,88] Moreover, this additional baseline normalization puts emphasis on a short-term variability of alpha changes right before the visual stimulus, previously shown to be perceptually relevant.[6,8,10,12,56] This procedure was applied separately for each participant. Mean alpha (7-13Hz) amplitude was computed in the cue-stimulus interval (-400 ms to stimulus presentation). The electrode within the contralateral parieto-occipital cluster with the most negative power was selected for alpha-amplitude analyses.

ERP data were analysed using custom routines in MatLab (Mathworks, Natic, MA) and EEGLAB. In line with previous studies, the P1 amplitude and latency were calculated at the most positive peak in a time window between 70 ms and 130 ms relative to the stimulus onset,[14] and at the same electrode as for the prestimulus alpha. The P300 was quantified as the mean amplitude between 100 ms and 500 ms relative to the stimulus onset at a centroparietal electrode (i.e., Cz).[89,90]

#### *Statistical Analyses*

In order to investigate the possible relationships between inter-subject differences in alpha oscillatory activity (prestimulus IAF and alpha amplitude), ERPs (latency/amplitude of P1 and latency/amplitude of P3), and behavior (task accuracy and confidence), non-parametric robust correlation estimates were used (skipped Pearson correlation). The advantage of this correlation coefficient is that it takes into account the presence of bivariate outliers (by excluding them) and thus is not sensitive to the presence of extreme values in the overall structure of the data.[91]

### Experiment 2

#### *EEG recordings –acquisition and processing*

EEG data were collected for Experiment 2 as for Experiment 1, with the only difference in higher sampling rate applied here (5000Hz instead of the 1000 Hz used in Experiment 1), as a higher sampling rate in online TMS-EEG protocols is strongly advised.[92]

Additional processing steps included cutting and interpolating (cubic interpolation) time points around the TMS pulses, as well as performing Indipendent Component Analysis (ICA) to deal with potential artifacts. Specifically, a fastICA algorithm is used (pop_tesa_fastica function) to identify individual components representing artifacts, along with automatic component classification (pop_tesa_compselect function),[93] where each component should be subsequently manually checked and reclassified when necessary (for more details, see [44]).

For the subsequent analysis of the ERPs, only correct trials with stimuli contralateral to the stimulation site (stimuli in LVF) were considered. The EEG data were then averaged across trials. Time windows for detecting peak amplitudes and their latencies were the same as per Experiment 1 (70–130 ms for the P1 and 100–500 ms for the P3). Likewise, the electrodes considered for P1 (O2, PO8, and PO4) and P3 (Cz) components were also kept constant across participants and the two experiments.

### *Statistical Analyses*

Differences in ERPs (P1 latency and P3 amplitude) were explored across three experimental GROUPS (IAF-1Hz, IAF and IAF+1Hz group) and the two STIMULATION protocols (TMS and SHAM stimulation) in a 2 × 3 repeated measures mixed-model ANOVAs. Subsequently, specific differences between conditions were tested via two-tailed t-tests (planned comparisons).